Video Article

# Paramyxoviruses for Tumor-targeted Immunomodulation: Design and Evaluation Ex Vivo

Johannes P.W. Heidbuechel[1,2], Christine E. Engeland[1,3]

[1]Department of Translational Oncology, German Cancer Research Center (DKFZ) and National Center for Tumor Diseases (NCT)

[2]Faculty of Biosciences, Heidelberg University

[3]Department of Medical Oncology, NCT and Heidelberg University Hospital

Correspondence to: Christine E. Engeland at christine.engeland@nct-heidelberg.de

URL: https://www.jove.com/video/58651
DOI: doi:10.3791/58651

Keywords: Oncolytic virotherapy, cancer immunotherapy, viral vectors, measles virus, paramyxovirus, bispecific T cell engager

Date Published: 12/11/2018

Citation: Heidbuechel, J.P., Engeland, C.E. Paramyxoviruses for Tumor-targeted Immunomodulation: Design and Evaluation Ex Vivo. *J. Vis. Exp.* (), e58651, doi:10.3791/58651 (2018).

## Abstract

Successful cancer immunotherapy has the potential to achieve long-term tumor control. Despite recent clinical successes, there remains an urgent need for safe and effective therapies tailored to individual tumor immune profiles. Oncolytic viruses enable the induction of anti-tumor immune responses as well as tumor-restricted gene expression. This protocol describes the generation and ex vivo analysis of immunomodulatory oncolytic vectors. Focusing on measles vaccine viruses encoding bispecific T cell engagers as an example, the general methodology can be adapted to other virus species and transgenes. The presented workflow includes the design, cloning, rescue, and propagation of recombinant viruses. Assays to analyze replication kinetics and lytic activity of the vector as well as functionality of the isolated immunomodulator ex vivo are included, thus facilitating the generation of novel agents for further development in preclinical models and ultimately clinical translation.

## Video Link

The video component of this article can be found at https://www.jove.com/video/58651/

## Introduction

Oncolytic viruses (OVs) are being developed as anti-cancer therapeutics that specifically replicate within and kill tumor cells while leaving healthy tissues intact. It has now become common understanding that oncolytic virotherapy (OVT), in most cases, does not rely solely on complete tumor lysis by efficient replication and spreading of the virus, but requires additional mechanisms of action for treatment success, including vascular and stromal targeting and, importantly, immune stimulation[1,2,3,4]. While many early OV studies used unmodified viruses, current research has profited from an improved biological understanding, virus biobanks that potentially contain novel OVs, and the possibilities offered by genetic engineering in order to create advanced OV platforms[5,6,7].

Given the recent success of immunotherapy, immunomodulatory transgenes are of particular interest regarding the genetic engineering of OVs. Targeted expression of such gene products by OV-infected tumor cells reduces toxicity compared to systemic administration. Targeting is achieved either by using viruses with inherent oncoselectivity or by modifying viral tropism[8]. Local immunomodulation enhances the multi-faceted anti-tumor mechanisms of OVT. Furthermore, this strategy is instrumental in interrogating the interplay between viruses, tumor cells, and the host immune system. To this end, this protocol provides an applicable and adjustable workflow to design, clone, rescue, propagate, and validate oncolytic paramyxovirus (specifically measles virus) vectors encoding such transgenes.

Modulation of the immune response can be achieved by a wide variety of transgene products targeting different steps of the cancer-immunity cycle[9], including enhancing tumor antigen recognition [e.g., tumor-associated antigens (TAAs) or inducers of major histocompatibility complex (MHC) class I molecules] over supporting dendritic cell maturation for efficient antigen presentation (cytokines); recruiting and activating desired immune cells such as cytotoxic and helper T cells [chemokines, bispecific T cell engagers (BTEs)]; targeting suppressive cells such as regulatory T cells, myeloid-derived suppressor cells, tumor-associated macrophages, and cancer-associated fibroblasts (antibodies, BTEs, cytokines); and preventing effector cell inhibition and exhaustion (checkpoint inhibitors). Thus, a plethora of biological agents is available. Evaluation of such virus-encoded immunomodulators regarding therapeutic efficacy and possible synergies as well as understanding of respective mechanisms is necessary to improve cancer therapy.

Negative sense single-stranded RNA viruses of the *Paramyxoviridae* family are characterized by several features conducive to their use as oncolytic vectors. These include a natural oncotropism, large genomic capacity for transgenes (more than 5 kb)[10,11], efficient spreading including syncytia formation, and high immunogenicity[12]. Therefore, OV platforms based on canine distemper virus[13], mumps virus[14], Newcastle disease virus[15], Sendai virus[16,17], simian virus 5[18], and Tupaia paramyxovirus[19] have been developed. Most prominently, live attenuated measles virus vaccine strains (MV) have progressed in preclinical and clinical development[20,21]. These virus strains have been used for decades for routine immunization with an excellent safety record[22]. Moreover, there is no risk for insertional mutagenesis due to the strictly

 

cytosolic replication of paramyxoviruses. A versatile reverse genetics system based on anti-genomic cDNA which allows for insertion of transgenes into additional transcription units (ATUs) is available[11,23,24]. MV vectors encoding sodium-iodide symporter (MV-NIS) for imaging and radiotherapy or soluble carcinoembryonic antigen (MV-CEA) as a surrogate marker for viral gene expression are currently being evaluated in clinical trials (NCT02962167, NCT02068794, NCT02192775, NCT01846091, NCT02364713, NCT00450814, NCT02700230, NCT03456908, NCT00408590, and NCT00408590). Safe administration has been confirmed and cases of anti-tumor efficacy have been reported in previous studies[25,26,27,28,29,30] (reviewed by Msaouel *et* al.[31]), paving the way for additional oncolytic measles viruses that have been developed and tested preclinically. MV encoding immunomodulatory molecules targeting diverse steps of the cancer-immunity cycle have been shown to delay tumor growth and/or prolong survival in mice, with evidence for immune-mediated efficacy and long-term protective immune memory in syngeneic mouse models. Vector-encoded transgenes include granulocyte-macrophage colony stimulating factor (GM-CSF)[32,33], *H. pylori* neutrophil-activating protein[34], immune checkpoint inhibitors[35], interleukin-12 (IL-12)[36], TAAs[37], and BTEs[38], which cross-link a tumor surface antigen with CD3 and thus induce anti-tumor activity by polyclonal T cells, irrespective of T cell receptor specificity and co-stimulation (**Figure 1**). The promising preclinical results obtained for these constructs demand further translational efforts.

Talimogene laherparepvec (T-VEC), a type I herpes simplex virus encoding GM-CSF, is the only oncolytic therapeutic approved by the United States Food and Drug Administration (FDA) and European Medicines Agency (EMA). The phase III study leading to approvals in late 2015 has not only shown efficacy at the site of intra-tumoral injection, but also abscopal effects (i.e., remissions of non-injected lesions) in advanced melanoma[39]. T-VEC has since entered additional trials for application in other tumor entities (e.g., non-melanoma skin cancer, NCT03458117; pancreatic cancer, NCT03086642) and for evaluation of combination therapies, especially with immune checkpoint inhibitors (NCT02978625, NCT03256344, NCT02509507, NCT02263508, NCT02965716, NCT02626000, NCT03069378, NCT01740297, and Ribas *et* al.[40]).

This demonstrates not only the potential of oncolytic immunotherapy but also the need for further research to identify superior combinations of OVT and immunomodulation. Rational design of additional vectors and their development for preclinical testing is key to this undertaking. This will also advance understanding of underlying mechanisms and has implications for the progression towards more personalized cancer treatment. To this end, this publication presents the methodology for the modification and development of paramyxoviruses for targeted cancer immunotherapy and, more specifically, of oncolytic measles viruses encoding T cell-engaging antibodies (**Figure 2**).

## Protocol

**NOTE:** [O], [P], and [M] indicate subsections applicable to: OVs in general, (most) paramyxoviruses, or MV only, respectively. [B] indicates sections specific for BTE transgenes.

# 1 Cloning of Immunomodulator-encoding Transgenes into Measles Virus Vectors

1. **[O] Design insert sequence.**
    1. [O] Decide on an immunomodulator of interest based on literature research or on exploratory data such as genetic screens[41] and derive the relevant cDNA sequence from appropriate databases such as GenBank, the European Nucleotide Archive, or the international ImMunoGeneTics information system (IMGT).
    2. [O] Add additional features to the transgene sequence (**Figure 3**). A preceding Kozak sequence and species-specific codon optimization can enhance expression. Signal sequences are required for secretion. Include sequences encoding N- and/or C-terminal protein tags for detection and purification[42]. Include restriction sites for insertion into the vector.
    **NOTE:** [M] Additional transcription units (ATUs) harboring MV polymerase gene start and stop signals are necessary for transgene expression from recombinant MV genomes. Suitable anti-genomic cDNA vectors, controlled by CMV promoters and containing ATUs with unique restriction sites for introduction of positive sense transgenes at defined positions, have been developed previously[11].
    [P] Adequate positioning of the transgene is crucial, as it affects viral replication and transgene expression due to the expression gradient typical for paramyxoviruses[43]. Introduction into an ATU close to the 3' end of the anti-genome (i.e., in the leader position or downstream of the *P* gene) generally results in high transgene expression at the cost of reduced viral replication. Increased replication and lower levels of transgene expression can be expected when using the ATU downstream of the *H* gene. Packaging of the genome of several paramyxoviruses, including measles virus, requires binding of six nucleotides by each nucleocapsid protein[44]. For insertion of transgenes into such viruses, ensure that the number of nucleotides of the complete genome will be divisible by six. This is also referred to as "rule of six"[45,46]. If necessary, include additional nucleotides in the insert (upstream of the Kozak sequence or downstream of the stop codon) without introducing frame shifts or premature stop codons. [M] Avoid particular sequences in the transgene that are similar to MV gene start (AGGRNCMARGW) and stop (RTTAWANAAAA) signals and RNA editing sequences (AAAAAGGG). Such consensus sequences have been published (e.g., see Parks et al.[47]).
    3. [O] Purchase oligonucleotide of the desired sequence or assemble from available sequences using standard molecular cloning[48].
    **NOTE:** [O] For PCR amplification of the transgene, design a forward primer including the upstream restriction site and the first 15-20 nucleotides of the insert and a reverse primer including the last 15-20 nucleotides of the insert followed by the downstream restriction site.

2. **[O] Clone insert into DNA encoding the viral (anti-)genome.**
    1. [O] Clone the insert into DNA vectors or DNA anti-genomes of RNA viruses by standard molecular cloning techniques[48] (i.e., enzymatic restriction followed by DNA ligation).
        1. [O] Prevent re-ligation of the vector by using non-compatible restriction sites or by de-phosphorylation prior to ligation.
        2. [O] Isolate the ligation product by agarose gel electrophoresis and subsequent gel purification using commercially available kits. In general, optimal ligation efficiency is achieved at a 3:1 molar ratio of insert to vector.
    2. [O] Transform the ligation product into competent bacteria suited for efficient recovery of large plasmids (i.e., perform heat shock of *E. coli*[49]) and identify bacterial clones harboring the correct DNA by colony PCR[50].

3. [O] Isolate amplified DNA from a single bacterial clone using commercially available DNA preparation kits. Confirm genomic integrity by control digest with appropriate restriction enzymes (e.g., HindIII for MV genomes [M]). Confirm correct insertion and integrity of the transgene by sequencing.
**NOTE:** [M] For transgenes inserted in the MV *H*-ATU, perform Sanger sequencing with the following primers: H-9018 [forward primer, binds to MV genome position 9018 in the *H* open reading frame (ORF)]: 5' GTGTGCTTGCGGACTCAGAATC 3'; L-9249+ (reverse primer, binds to MV genome position 9249 in the *L* ORF): 5' CAGATAGCGAGTCCATAACGG 3'.

## 2. Rescuing Recombinant Measles Virus Particles Encoding Immunomodulators

1. **[O] Generate recombinant virus particles from (anti-)genomic DNA *via* transfection of virus producer cells according to the standard protocol for the respective virus. Follow guidelines for working under sterile conditions. Perform cell culture under hoods, in particular all steps involving virus in class II biological safety cabinets.**
    1. [M] For rescue of measles viruses from cDNA[23,24], plate MV producer (African green monkey kidney-derived Vero) cells evenly on a 6-well plate 24 h before transfection. Seed 2 x $10^5$ cells in 2 mL Dulbecco's Modified Eagle's Medium (DMEM) containing 10% fetal bovine serum (FBS) per well to achieve 65–75% confluency at the time of transfection.
    **NOTE:** [P] Reduce cell numbers if the cells overgrow prior to virus-induced syncytia formation.
    2. [P] Transfect the cells with DNA encoding the viral anti-genome, required helper plasmids, and, if desired, a plasmid encoding a fluorescent reporter to assess transfection efficiency.
        1. [M] Mix 5 µg of recombinant DNA encoding the measles virus anti-genome, 500 ng each of mammalian expression plasmids encoding measles virus N and L proteins, and 100 ng each of plasmids encoding P protein and a fluorescent reporter in a total volume of 200 µL DMEM.
        2. Add 18.6 µL of liposomal transfection reagent, immediately mix by flicking the tube, and incubate for 25 min at room temperature (RT).
        3. [P] Replace the medium with 1.8 mL of DMEM, 2% FBS, 50 µg/mL kanamycin (or other antibiotics to prevent contamination) per well, then add the transfection mix dropwise to the well and swirl carefully. Incubate cells overnight at 37 °C, 5% $CO_2$. Replace medium with 2 mL of fresh DMEM, 2% FBS, and 50 µg/mL kanamycin the next day; repeat this when medium becomes acidic.
        **CAUTION:** [O] Handle cells and materials according to biosafety regulations, as virus may be present from transfection through the following steps. Dispose of (potentially) infectious waste appropriately.

2. **[P] Collect and propagate virus particles.**
    1. [P] Observe cells daily by microscopy for reporter gene expression and syncytia formation (**Figure 4**). Harvest virus when large syncytia, consisting of 20 or more cells, are visible, or when cells become too dense (i.e., when they start to grow in multiple layers, typically after 7–9 days).
    **NOTE:** [P] If no syncytia are observed for a given vector construct, this does not necessarily mean that the rescue has failed. As infectious virus may nevertheless be present in the sample, transfer to fresh producer cells for passaging.
    2. [P] Seed approximately 1.5 x $10^6$ producer cells in 12 mL of DMEM with 10% FBS, on 10 cm dishes 24 h before the anticipated harvest, or 2.5 x $10^6$ cells per plate 4–6 h prior to passaging of the virus to achieve 65-75% confluency at the time of virus inoculation.
    3. [P] To collect virus progeny, carefully scrape adherent producer cells from the plate using a cell scraper and transfer the supernatant containing cells into a centrifuge tube. Remove cell debris by centrifugation for 5 min at 2,500 x *g* and 4 °C.
    **NOTE:** Scraped cells may be transferred directly without centrifugation to maximize virus carryover at the cost of suboptimal culture conditions and potential microscopy artifacts.
    **CAUTION**: [O] Avoid spilling media when scraping cells. Minimize aerosol formation.
    4. [P] Prepare inoculum by mixing the cell-free supernatant from step 2.2.3 with serum-free medium to a final volume of 4 mL. Replace the medium on producer cells by the inoculum and incubate cells for at least 2 h at 37 °C and 5% $CO_2$. Add 6 mL of DMEM with 10% FBS and incubate cells overnight before changing the medium to 12 mL of fresh DMEM with 10% FBS.
    5. [P] Observe the cells at least twice daily and harvest virus before syncytia burst (i.e., when membrane disruption becomes visible). To harvest the first passage of virus, remove supernatant from the plate, add 600 µL of serum-free medium, scrape cells with a cell lifter, and transfer to a clean tube.
    **NOTE:** [M] Depending on virus strain[51,52] and progression of infection, transfer plates with infected cells to 32 °C to facilitate viral replication and spread. In general, MV Schwarz strains propagate well at 37 °C, while transfer of cells infected with Edmonston B strain viruses to 32 °C results in slower syncytia formation but higher titers.
    **NOTE:** [P] Do not allow the cell layer to dry during harvest, as this will result in reduced infectivity of viral particles. Although some virus is lost when discarding the supernatant of infected cells, higher titers can be obtained from the cell layer.
    6. [P] Immediately freeze the virus suspension in liquid nitrogen. Store at -80 °C for at least 24 h to ensure thorough freezing. Extend to several days to interrupt the procedure, if needed.
    7. Release viral particles by thawing at 37 °C. Homogenize by vortexing, and centrifuge for 5 min at 2,500 x *g* and 4 °C. Transfer the supernatants to labeled cryotubes and store at -80 °C.
    **NOTE:** [O] Store viruses in aliquot sizes adequate for later experiments, as they are preferentially thawed only once and used immediately. [P] Further freeze-thaw cycles or storage at 4 °C over several days result in significant reduction of viral titers.
    8. [P] One day prior to further passaging to achieve required amount and titer, seed 4 x $10^6$ producer cells in 12 mL of DMEM with 10% FBS on 15 cm dishes. Inoculate with virus at a multiplicity of infection (MOI) of 0.03. Infect in 8 mL of serum-free medium per plate and change medium to DMEM with 10% FBS after incubating cells for at least 2 h. Scale up by using multiple plates.
    9. Harvest as described in step 2.2.5, when syncytia have spread across the whole cell layer. Pool the obtained suspensions in 50 mL tubes and process as described in steps 2.2.6–2.2.7.
    **NOTE:** [O] It is crucial to check all plates visually for bacterial and fungal contamination before harvesting. In general, check all cell lines regularly for contamination with mycoplasma or adventitious viruses by multiplex PCR.

3. **[P] Evaluate viral titers.** Determine titers of virus stocks in octuplicates per aliquot using 96-well plates. Perform titration of three individual aliquots per virus rescue and use the average value to calculate the amount of virus suspension to be used in experiments.
    1. [P] Pool the producer cells, count, and adjust to 1.5 x $10^5$ cells per mL in DMEM with 10% FBS.
    2. [P] Pipet 90 µL of DMEM with 10% FBS into each well of a 96-well plate.
    3. [P] Add 10 µL from one aliquot of the virus stock to all 8 wells in the first column of the plate and mix thoroughly by pipetting up and down at least 10 times.
    4. [P] Perform serial 10-fold dilutions of the virus. Transfer 10 µL of each well from the first to the second column using a multichannel pipet. Mix thoroughly by pipetting up and down and use fresh pipet tips for each dilution step. Discard 10 µL from each well of the last column.
    **NOTE:** Each 96-well plate allows for 12 serial dilution steps. [M] For MV vectors, 8 steps of 10-fold dilutions are typically sufficient, as titers above 1 x $10^9$ cell infectious units (ciu)/mL are rarely obtained by the method of propagation described in step 2.2. [P] Control wells without virus can be used for comparison and to monitor contamination.
    5. [P] Add 100 µL of cell suspension to each well and incubate at 37 °C, 5% $CO_2$ for 48 h. Ensure the absence of cell clumps in the suspension to achieve homogenous distribution of cells.
    6. [P] Check for syncytia using a light microscope. Count syncytia in each well of the column with the highest dilution factor containing visible syncytia.
    7. [P] Calculate the average number of syncytia per well in that column by dividing the total number of syncytia by eight. Multiply that average with the dilution factor of the respective column, starting at $10^2$ ciu per mL for the first column[53] (see **Figure 5** as an example).

## 3. Determining Replicative and Cytotoxic Capacities of Viral Vectors Encoding Immunomodulators

1. **[O] Compare replication kinetics of the generated recombinant virus and the unmodified vector with one-step or multi-step growth curves (GCs). For one-step GCs, viral progeny are assessed following simultaneous infection of all cells (theoretically, 100% infection). Multi-step GCs start at a low percentage of infected cells to follow several rounds of virus replication.**
    1. [M] For analysis of measles virus replication kinetics, seed 1 x $10^5$ Vero cells in 1 mL of DMEM with 10% FBS per well on 12-well plates one day prior to infection. Plate at least two wells for each timepoint of interest as technical replicates.
    2. [O] Infect the cells with virus at low MOI for multi-step or at high MOI for one-step GCs [M] (0.03 and 3 for MV replication on Vero cells, respectively). Replace medium with 300 µL of serum-free medium containing the respective amount of virus and incubate at 37 °C and 5% $CO_2$ for at least 2 h. Remove inoculum, add 1 mL of DMEM with 10% FBS, and continue incubation.
    3. [P] At relevant timepoints such as 12, 24, 36, 48, 72, and 96 h after infection, harvest viral progeny by directly scraping cells into the medium. Transfer contents from each well to an individual tube, snap-freeze in liquid nitrogen and store at -80 °C until titration.
    **NOTE:** [P] Replicate samples may be pooled at this step for analysis of average titers.
    4. [P] Collect samples from all timepoints. Thaw simultaneously at 37 °C for assessment of viral progeny. Vortex and pellet cell debris by centrifugation for 5 min at 2,500 x *g* and 4 °C.
    5. [P] Calculate average titers of each construct and timepoint as described above. Plot titers over time. Compare growth curves of vectors with and without inserted transgenes, with different transgenes, or with transgenes inserted at different positions (see **Figure 6A**).

2. **[O] Compare lytic activities of immunomodulator-encoding and unmodified viruses.**
    1. [O] Select from possible methodologies including impedance measurements, lactate dehydrogenase (LDH) release assay, or metabolism-based colorimetric cell viability assays [e.g., 3-(4,5-dimethylthiazol-2-yl)-2,5-diphenyltetrazolium (MTT) and 2,3-bis-(2-methoxy-4-nitro-5-sulfophenyl)-2H-tetrazolium-5-carboxanilide (XTT) assays].
        1. [M] To analyze cytotoxicity of measles virus vectors using XTT assay, seed Vero cells as described in step 3.1.1. Include replicates of a non-infected control for each timepoint.
        **NOTE:** [O] Performing XTT assay at different timepoints on the same sample can limit technical errors, but repeated washing and exposure to XTT reagent affects numbers of viable cells. Impedance provides an alternative readout for continuous measurements.

    2. [M] Infect Vero cells at an MOI of 1 as described in step 3.1.2.
    **NOTE:** [M] For infection of less permissive target cells such as some murine tumor cell lines, a higher MOI of 3 or 5 may be necessary.
    3. [O] At timepoints of interest (e.g., 12, 24, 36, 48, 72, and 96 h after infection) prepare the required amount of XTT reagent (i.e., 300 µL per well plus 10% excess). Avoid light exposure.
    4. [M] At each timepoint, remove medium from respective wells. Replace by 300 µL of XTT reagent and incubate at 37 °C in the dark. Collect supernatants when the reagent in the control wells has turned deep red, which typically takes between 15 min and 2 h, and freeze at -20 °C.
    **NOTE:** [O] Incubation times depend on virus construct, cell type, density, and cytopathic effect.
    5. [O] After collecting all samples, thaw simultaneously. Transfer 100 µL of each sample to a 96-well plate and measure optical absorbance at 450 nm, with 630 nm as a reference wavelength.
    6. [O] Plot timepoints (x-axis) vs. optical absorbance of samples relative to controls, indicating metabolic activity as a surrogate for cell viability (y-axis). Decreasing relative absorbance over time implies viral cytotoxicity (see **Figure 6B**).

## 4. Analyzing Activity of Virus-encoded Immunomodulators Secreted from Infected Cells

1. **[O] Isolate secreted transgene products expressed by virus-infected target cells.**
    1. [P] Let virus producer cells grow to 70% confluency in T175 flasks.

2. [P] Remove medium from cells and wash twice with 12 mL of PBS to remove serum. Inoculate cells with virus at an MOI of 0.03 in 12 mL of serum-free medium and incubate at 37 °C and 5% $CO_2$ overnight. Replace medium with 12 mL of fresh serum-free medium.
    1. [M] For Edmonston B viruses, transfer cells from 37 to 32 °C after 40 h for another 24 h of incubation to facilitate infection and prevent premature bursting of syncytia. Depending on virus strain[51,52] and syncytia progression, incubation temperatures and times may be adjusted for optimal protein yield and purity.

3. [P] Carefully collect supernatants without detaching cells before syncytia burst. Optimally, syncytia have spread across the entire cell layer. Pool supernatants in 50 mL tubes.
   **NOTE:** [P] For efficient purification of the transgene product, avoid bursting of syncytia and minimize cell debris when harvesting the supernatants of infected cells.
4. [P] Remove cell debris from the supernatant by centrifugation for 5 min at 2,500 x *g* and 4 °C and passing through 0.22 µm filters. Depending on the total volume of the filtrate, this can be performed using a syringe or a vacuum pump.
5. [O] Isolate transgene product using an appropriate purification method. Purify proteins with a hexa-histidine (His) tag by affinity exchange chromatography using Ni-NTA mini spin columns[38] as described here in brief (steps 4.1.5.1–4.1.5.4).
   **NOTE:** [O] Perform all steps fast and on ice. Pre-chill buffers and pre-cool centrifuge to 4 °C.
    1. [O] Prepare 100 mL each of buffer with PBS, 200 mM sodium chloride and imidazole at final concentrations of 10 mM (washing buffer 1, WB1), 20 mM (washing buffer 2, WB2), and 500 mM (elution buffer, EB). Adjust pH of WB1 and WB2 to 8.0 and of EB to 7.0. Depending on the protein to be purified, imidazole concentrations may have to be adjusted.
    2. [O] Equilibrate columns with 600 µL of WB1 and centrifuge at 800 x *g* for 2 min with an open lid.
    3. [O] Load 600 µL of filtered supernatants onto columns. Allow binding of His-tagged proteins to the column matrix by centrifugation at 200 x *g* for 5 min with a closed lid. Loading and binding can be repeated up to a total of 300 µg His-tagged protein per column.
    4. [O] Wash thrice with WB1 and once with WB2, or until the flow-through is colorless. Add 600 µL of buffer and spin at 800 x *g* for 2 min with open lid.
    5. [O] Elute protein into a fresh tube by performing two elution steps with 300 µL of EB and centrifugation for 2 min at 800 x *g*.
    6. [O] Desalt and concentrate product using centrifugal filters according to product size. Add PBS to a volume of 15 mL and filter *via* centrifugation for 10 min at 4,000 x *g*. Repeat until the desired purity and concentration is achieved. To increase protein concentration, reduce the final volume to approximately 200 µL by centrifugation for 40 min at 4,000 x *g*.

2. **[O] Confirm purity and identity of the product.**
    1. [O] Quantify the amount of total protein in the isolates using standard colorimetric assays such as bicinchoninic acid (BCA) or Bradford assay[54,55]. [M] Typical values can range from 1–3 µg transgene product per mL supernatant of infected cells.
    2. [O] For relative quantification of protein isolates, separate *via* sodium dodecyl sulfate polyacrylamide gel electrophoresis (SDS-PAGE) and perform Coomassie staining[56].
    3. [O] Confirm identity of the purified products by immunoblotting using specific antibodies targeting the protein or an associated peptide tag[57].
    4. [O] Analyze protein binding specificity using appropriate techniques that may include enzyme-linked immunosorbent assay (ELISA) or flow cytometry (see **Figure 7**). Cell binding can be confirmed using a recently described magnetic pulldown assay[38].
       **NOTE:** [O] Use appropriate controls. In cell binding assays, include negative controls with cells not expressing the targeted molecule (as in **Figure 9**) and non-targeting protein surrogates (**Figure 8**). In flow cytometry experiments, include positive, negative and isotype controls (**Figure 7**).
        1. [O] Co-incubate the target cells and protein isolate to allow binding. [B] For binding analysis of BTEs to peripheral blood mononuclear cells (PBMCs) isolated from human blood[58], incubate 2.5 x $10^6$ cells with 200 ng of BTE in 100 µL of PBS with 1% FBS (binding buffer, BB) for 1 h on ice.
        2. [B] Wash cells with 1 mL of BB to remove unbound protein. Centrifuge at 300 x *g* for 5 min, discard supernatant, and resuspend pellet in 100 µL of BB. Add biotinylated antibody targeting either the protein of interest or an associated peptide tag and incubate on ice for 30 min. For BTEs with influenza hemagglutinin (HA) tag, use 100 ng of anti-HA-Biotin (clone 3F10).
        3. [B] Wash cells twice with 1 mL of BB and resuspend in 80 µL of BB. Add 20 µL of streptavidin-coupled magnetic microbeads and incubate for 15 min at 4 °C.
        4. [B] Wash once to remove excess beads and resuspend pellet in 500 µL of BB supplemented with 2 mM EDTA (column buffer, CB).
        5. [B] Isolate cells with columns and a magnetic stand according to the provider's manual.
            1. [B] Equilibrate by allowing 500 µL of CB to pass through the column by gravity flow.
               **NOTE:** [B] The column must never run dry. Pipet carefully and degas the buffers to avoid bubbles.
            2. [B] Place a clean tube under the column and apply the cell/bead suspension to the column. Wash the column three times with 500 µL of CB per wash. Collect flow-through samples of the suspension and of at least the first washing step in the tube, then store on ice.
            3. [B] Elute bead-bound cells retained by the magnetic field. To this end, remove the column from the magnetic stand, place it over a clean tube, add 1 mL of CB, and quickly push the buffer through the column into the tube using a plunger. Keep the tube on ice.

        6. [B] Centrifuge tubes containing flow-through and elution samples for 20 min at 16,000 x *g* and 4 °C to pellet cells. Discard supernatants and lyse cells in a radioimmunoprecipitation assay (RIPA) buffer (suggested: 75 µL). Perform SDS-PAGE[56].
        7. [B] Perform immunoblotting using a suitable primary antibody. Antibodies may target the transgene product or a cellular protein (e.g., β-actin, **Figure 8**) to assess BTE-cell binding.

3. **[O] Assess immunological functionality of isolated immunomodulators.**
    1. [O] Identify relevant assays according to the characteristics of the encoded immunomodulator. Regarding the expected immunomodulatory activity, methods assessing cell proliferation, migration, maturation, activation, or cytotoxicity may be applied.

**NOTE:** [O] Cell proliferation can be analyzed by CFSE[59] labeling or Ki67 staining[60]. Transwell or scratch experiments are available to analyze cell migration[61]. Maturation and activation of cells can be assessed using appropriate staining protocols for respective markers. [B] Available techniques to assess BTE-mediated cellular cytotoxicity include impedance measurements and chromium release assay. If opting for chromium release assay, observe proper safety measures when handling radioactive material.

2. [B] As a non-radioactive alternative, the following describes in detail how to evaluate BTE-induced, cell-mediated cytotoxicity by LDH release assay (described previously in brief[38]).
    1. [B] Decide on conditions to be tested during the experiment (see **Figure 9** as an example). Timepoints (hours to days), concentrations of the immunomodulator (pg/mL to µg/mL) and effector to target cell (E:T) ratios (between 1:50 and 50:1, for example) can be varied. Always prepare samples in triplicates.
    2. [B] Include samples without protein and without effector cells, controls for spontaneous LDH release of the single cell types ($T_{sp}$ and $E_{sp}$), a target cell maximum lysis control ($T_{max}$) with detergent added before readout, a medium only control, and a volume control for $T_{max}$.
    **NOTE:** [B] Required numbers of target cells and incubation times can vary. Perform initial test runs without effector cells and immunomodulators to identify optimal parameters. Include $T_{sp}$ and $T_{max}$ samples and corresponding controls to assess different cell numbers and timepoints.
    3. [B] Isolate immune effector cells (e.g., by density gradient centrifugation of human blood to obtain PBMCs[58] or negative selection of murine T cells from mouse splenocytes[62]).
    4. [B] Seed target cells according to step 4.3.2 (e.g., 5 x $10^3$ per well) in a U-bottom 96-well plate.
    5. [B] Add the isolated protein at desired concentrations to the respective samples. Add immune effector cells at desired ratios. Add medium to a total volume of 100 µL per well.
    6. [B] Incubate for the time frame determined in step 4.3.2, typically between 4 and 48 h (24 h for unstimulated PBMCs and 48 h for freshly isolated murine T cells; shorter incubation times can apply for prestimulated immune cells), at 37 °C and 5% $CO_2$.
    7. [B] 45 minutes before collecting the samples, add 10 µL of 10x lysis solution to wells containing $T_{max}$ samples and the corresponding medium controls. Continue incubation.
    8. [B] Spin down cells at 250 x *g* for 4 min. Transfer 50 µL of each supernatant to a flat-bottom 96-well plate. Do not transfer cells to avoid cell-bound LDH.
    9. [B] Prepare substrate solution according to the manufacturer. Add 50 µL to each well and incubate at RT in the dark for 30 min or until $T_{max}$ samples turn deep red.
    10. [B] Add 50 µL of stop solution to each well. Remove air bubbles by centrifugation for 1 min at 4,000 x *g*, and manually with a hollow needle. Measure optical absorbance at 490 nm.
    11. [B] Calculate % specific lysis values for each sample.
        1. [B] Calculate averages for replicates of medium controls with and without lysis solution. Subtract obtained values from experimental samples and from $T_{max}$ and spontaneous release controls, respectively. Use these background-corrected values for further calculations.
        2. [B] Calculate averages for background-corrected $T_{max}$, $T_{sp}$, and $E_{sp}$ controls. Using these average values, the following equation yields the percentage of specific lysis for each sample:
        $$\frac{sample\ value - T_{sp} - E_{sp}}{T_{max} - T_{sp}} \times 100 = \%\ specific\ lysis$$
        3. [B] Plot % specific lysis values *vs.* protein concentration or E:T ratio and compare to the non-targeting control samples.

## Representative Results

**Figure 1** illustrates the mechanism of action of oncolytic measles viruses encoding bispecific T cell engagers. A flowchart depicting the workflow of this protocol is presented in **Figure 2**. **Figure 3** shows an example of a modified oncolytic measles virus genome. This provides a visual representation of the specific changes applied to the measles virus anti-genome and particular features of inserted transgenes. Typical measles virus-induced syncytia are depicted in **Figure 4**. Note the high cell density at the timepoint of harvesting the rescue (A, B), indicating that the cell number may be reduced when repeating the experiment. Incubation temperatures and -times may be optimized for passaging on Vero cells (C, D) to achieve improved spread of syncytia across the plate. **Figure 5** represents the outcome of a typical titration assay. In **Figure 6**, one-step growth curves (A) and relative cell viability (B) after inoculation with unmodified (MV) and BTE-encoding oncolytic measles viruses (MV-H-mCD3xhCD20) are shown. While growth curves of the compared vectors on Vero cells appear similar, lytic activity of the transgene-encoding virus lags behind in the murine tumor cell line. Flow cytometry data of target antigen-expressing cells incubated with BTEs at five different dilutions is provided in **Figure 7**, indicating BTE binding by cells in a concentration-dependent manner. **Figure 8** represents an exemplary immunoblot after magnetic pulldown of BTE-associated cells. Pulldown with non-targeting BTEs ($n_1$, $n_2$) did not yield detectable amounts of cells, whereas bands in the elution fraction, indicative of bound cells, were observed for targeting BTE samples ($t_1$, $t_2$). BTE-mediated, target antigen-specific and concentration-dependent cytotoxicity of murine T cells is indicated by a representative LDH release assay in **Figure 9**.

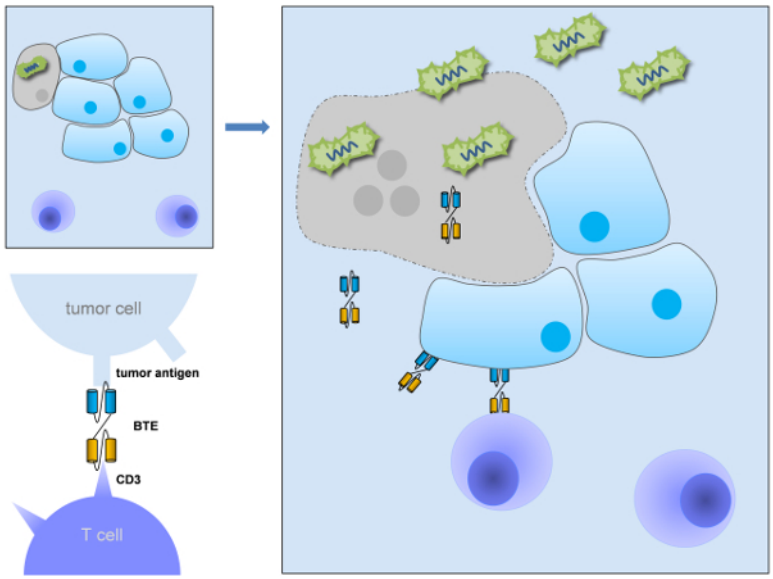


**Figure 1: Mechanism of action of oncolytic measles viruses encoding a bispecific T cell engager (MV-BTE).** Infection of a tumor cell (infected: grey, uninfected: light blue) with MV-BTE is followed by viral replication and spread throughout the tumor, resulting in tumor cell lysis and immune stimulation. Simultaneously, BTEs [consisting of two single chains derived from antibodies targeting CD3 on T cells (yellow) and a tumor surface antigen (blue)] are produced and secreted locally by virus-infected cells. BTE-mediated cross-linking with tumor cells induces activation of resting, polyclonal T cells, resulting in further tumor cell killing. Please click here to view a larger version of this figure.

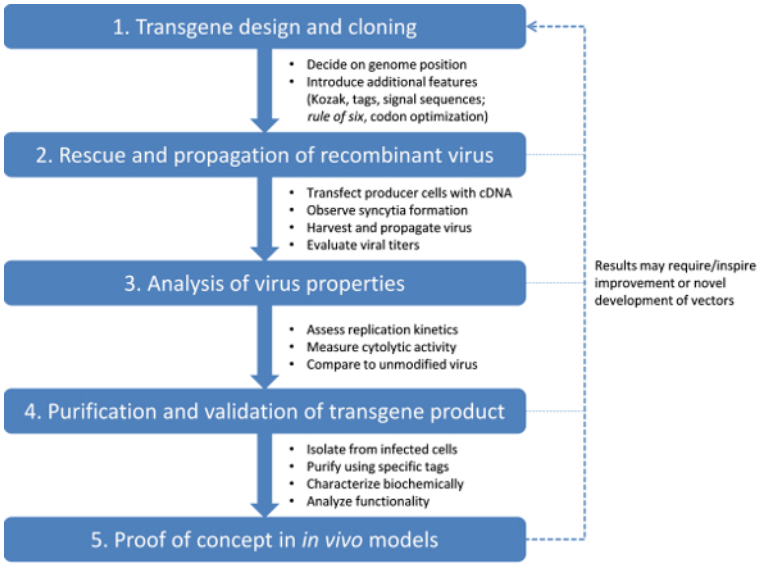


**Figure 2: Flowchart describing the workflow of designing, generating, and evaluating novel viral vectors encoding immunomodulatory transgenes.** Steps 1 to 4 reflect the respective sections of the protocol. Bullet points indicate relevant considerations and substeps. Due to the empirical nature of the procedure, adjustments or refinements can become necessary at any step of the workflow. In addition, experimental findings can lead to new hypotheses and inspire development of additional vectors or combination treatments. Please click here to view a larger version of this figure.

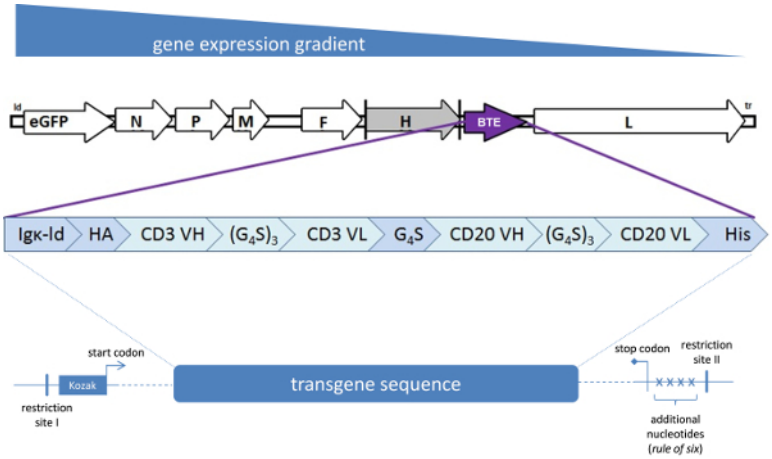


**Figure 3: Schematic representation of a measles virus genome.** Enhanced green fluorescent protein (eGFP) is encoded in an additional transcription unit downstream of the leader (ld) sequence. N, P, M, F, H, and L designate genes encoding the measles virus structural proteins nucleoprotein, P protein, matrix protein, fusion protein, hemagglutinin protein, and large protein (polymerase), respectively, which are differentially expressed as visualized above. A bispecific T cell engager (BTE) transgene is inserted into an additional transcription unit (ATU) downstream of the *H* open reading frame. The transgene encodes an Igκ leader peptide for efficient secretion as well as influenza hemagglutinin (HA) and hexa-histidine (His) protein tags for detection and purification. Genes coding for variable heavy (VH) and light chain (VL) domains of antibodies targeting CD3 and CD20, respectively, are connected *via* peptide linker sequences containing glycine (G) and serine (S) residues. The transgene sequence is preceded by a Kozak sequence. Downstream of the coding region, additional nucleotides have been included exemplarily to comply with the rule of six. The insert cassette is flanked by two restriction sites enabling insertion into the respective ATU. Please click here to view a larger version of this figure.

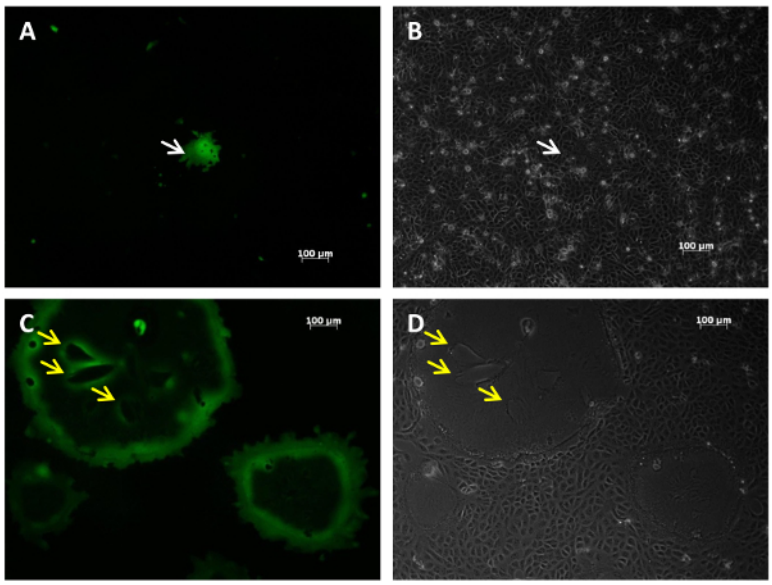


**Figure 4: Measles virus-induced syncytia.** (**A, B**) Vero cells were transfected with cDNA for rescue of recombinant measles viruses encoding enhanced green fluorescent protein (eGFP) and a bispecific T cell engager (BTE) targeting murine CD3 and human CD20. Presence of a fluorescent syncytium (white arrows) indicates successful rescue of infectious virus. (**C**, **D**) Measles viruses were harvested after rescue and propagated on Vero cells (passage 1). Large syncytia have formed and are already starting to burst (yellow arrows). Images were acquired by phase contrast (B, D) and fluorescence microscopy after excitation for 80 ms (A) and 100 ms (C). Please click here to view a larger version of this figure.

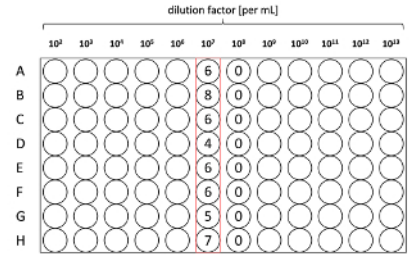


$$average\ number\ of\ syncytia = \frac{6+8+6+4+6+6+5+7}{8} = 6$$

$$titer = average\ number\ of\ syncytia\ x\ dilution\ factor = \mathbf{6\ x\ 10^7\ ciu/mL}$$

**Figure 5: Representative result of a titration assay.** Titration of a third-passage batch of MV-H-mCD3xhCD20, a BTE-encoding oncolytic measles virus, on Vero cells. A 10-fold serial dilution was performed on a 96-well plate, starting with 10 µL of virus suspension in each well of column 1.No syncytia were visible in column 7, as indicated by zeros. For the next lowest dilution of virus suspension in column 6, an average of six syncytia per well was observed, resulting in a final titer of approximately 6 x $10^7$ cell infectious units (ciu) per mL virus suspension. Please click here to view a larger version of this figure.

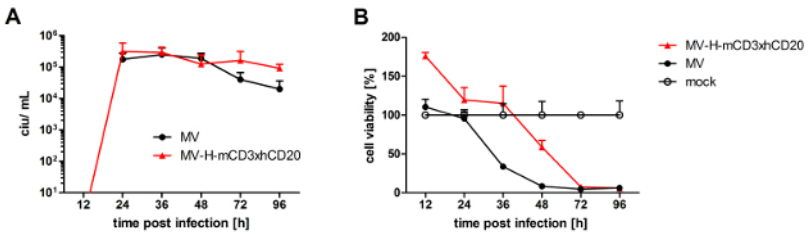


**Figure 6: Replication kinetics and lytic activity of recombinant measles viruses.** (**A**) One-step growth curves were generated after infection of Vero cells with unmodified oncolytic measles virus (MV) or measles virus encoding a bispecific T cell engager (MV-H-mCD3xhCD20) at an MOI of 1. Titers of viral progeny were evaluated at designated timepoints after infection, indicating similar virus replication kinetics. Means and standard deviations of eight samples (four technical replicates each of two biological replicates per timepoint) are shown. (**B**) Cell viability was assessed on MC38 murine colorectal carcinoma cells stably expressing human carcinoembryonic antigen and the MV receptor CD46 (MC38-CEA-CD46) after inoculation with medium only (mock) or indicated viruses at an MOI of 1. XTT cell viability assay was performed at indicated timepoints. Reduction in cell viability was observed at earlier timepoints for the unmodified vector. Values of over 100%, as calculated for MV-H-mCD3xhCD20 at the 12 h timepoint, are frequently observed shortly after infection, which may be due to cellular stress or cell-derived factors present in the virus suspension. Mean values plus standard deviations of three technical replicates are shown for each timepoint. Please click here to view a larger version of this figure.

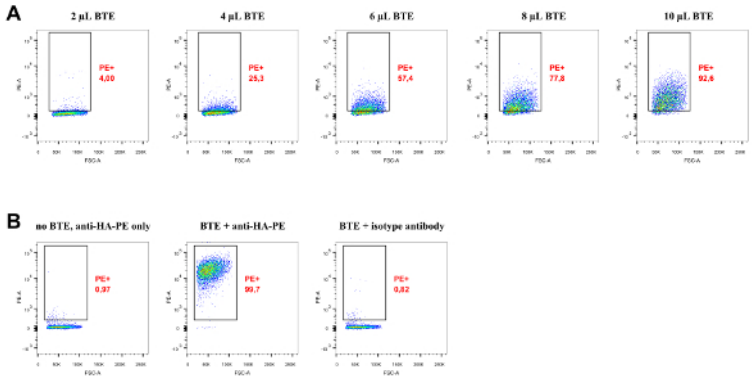


**Figure 7: Target cell binding by bispecific T cell engagers (BTEs) expressed from measles virus-infected cells.** Human mantle cell lymphoma cells endogenously expressing CD20 (Granta-519) were incubated with human immunoglobulin G to block Fc receptors, followed by incubation with 2, 4, 6, 8, or 10 µL (**A**) of purified mCD3xhCD20 BTE solution, respectively. BTE-bound cells were detected using phycoerythrin (PE)-conjugated antibody targeting the BTE-associated HA-tag. Percentages of stained cells correlated with BTE concentrations. (**B**) Controls for selectivity and specificity of binding. Shown here are controls from an independent experiment, including one sample each of cells not incubated with BTE but with the BTE-targeting antibody only (control for unspecific binding of antibody to cells) or with a BTE that is known to bind to the cells of interest, followed by incubation with either the BTE-targeting antibody (positive control) or an isotype antibody. If available, isogenic cells not expressing the target antigen of choice may be used to further verify binding selectivity. Please click here to view a larger version of this figure.

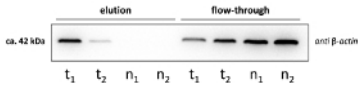


**Figure 8: Magnetic pulldown of human peripheral blood mononuclear cells (PBMCs) bound by measles virus-encoded BTEs.** Cells were incubated with two different batches of human T cell-targeting (t1, t2) or non-targeting control BTEs (n1, n2), respectively. BTE-bound cells were retained on columns using magnetic beads, pelleted, and lysed. β-actin in lysates was detected by immunoblotting. Intensities of bands in the elution samples indicate relative BTE-cell binding. Flow-through specimens confirm presence of cells in all samples. Please click here to view a larger version of this figure.

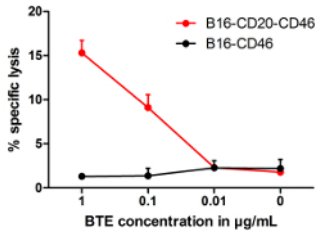


**Figure 9: Cytotoxic activity of measles virus-encoded BTEs.** Target tumor cells (5 x $10^3$ B16-CD20-CD46 cells per well) were incubated with murine T cells at a ratio of 1:50. BTEs previously purified from the supernatant of MV-H-mCD3xhCD20-infected cells were added at indicated concentrations. Relative lysis of target cells was assessed by LDH release assay after 48 h. Cells lacking the BTE target antigen (B16-CD46) served as reference to evaluate antigen-specific cytotoxicity. Means plus standard deviations of three technical replicates per sample are shown. Target antigen-expressing cells were specifically lysed in a BTE concentration-dependent manner. Purity of the BTE product and target antigen expression levels influence cell killing. In the present example, 15% specific cell killing was achieved at a relatively high BTE concentration of 1 µg/mL. This is a typical value for such an experimental setup with long co-incubation times and suboptimal T cell culture conditions. In other settings, up to 60% specific killing was achieved using BTEs purified from MV-infected supernatants, reaching a plateau at BTE concentrations of 100 ng/mL and higher[38]. This indicates that, counter-intuitively, the limit of this assay is less than 100% specific killing, which can be explained by different growth kinetics in $T_{max}$ controls compared to co-culture samples. Please click here to view a larger version of this figure.

## Discussion

Oncolytic immunotherapy (i.e., OVT in combination with immunomodulation) holds great promise for cancer treatment, demanding further development and optimization of oncolytic viruses encoding immunomodulatory proteins. This protocol describes methods to generate and validate such vectors for subsequent testing in relevant preclinical models and potential future clinical translation into novel anti-cancer therapeutics.

Numerous different oncolytic virus platforms with distinct advantages are available[63]. In addition to cancer specificity, vector safety, requirements for manufacturing, efficacy in tumor cell lysis, and induction of immune responses, cloning capacity is key for successful vectorization of immunomodulators using a specific oncolytic. Unfortunately, direct comparisons of different OVs are currently lacking and should be pursued in order to identify optimal treatment options for individual patients. This can be facilitated by promoting the rational development and testing of novel transgene-encoding vectors, as exemplified here for MV-BTE. Given the beneficial properties of MV (i.e., oncotropism, safety, fusogenicity, immunogenicity, feasibility of genetic modification) this protocol focuses on this oncolytic vector, which can be generalized for other OV, especially paramyxoviruses.

For a rational choice of potentially relevant immunomodulators as candidate transgenes (step 1.1.1), a thorough understanding of the cancer-immunity cycle is essential, making systematic literature research indispensable. In addition, large-scale screens, though costly, can prove valuable to identify novel targets (e.g., see Patel et al.[41]).

For design of recombinant OVs, desired expression profiles should be considered. In the case of RNA viruses, gene expression is controlled on the RNA level by the respective polymerase. When designing transgene cassettes for insertion into MV genomes (step 1.1.2), avoiding sequences that resemble MV polymerase gene start/stop signals and RNA editing sites and following the rule of six is crucial for successful vector development. Moreover, paramyxovirus gene expression levels correspond to positioning within the genome, resulting from an expression gradient[43]. In general, positioning of the transgene in an upstream position increases expression at the expense of reduced replication. However, these parameters also depend on the size, structure, and sequence of the respective transgene. Consequently, a limitation of the methodology described in this protocol is the need for empirical testing of novel vector designs. In specific cases, adjustments to the transgene sequence or positioning may be necessary to achieve desired vector characteristics (**Figure 2**). Systematic comparison of different positions for checkpoint antibody inserts showed optimal results for the *H*-ATU (unpublished data). As BTE inserts have comparable properties (size and immunoglobulin domains), MV-BTE vectors were cloned analogously[38].

Rescue of infectious particles from virus cDNA (step 2.1) may require several attempts for some constructs. Adjusting cell numbers can optimize cell density for syncytia formation. While a certain density is necessary for efficient cell-to-cell spread and fusion of cell membranes, contact inhibition reduces viral replication. Further, the number of infectious particles may not be sufficient to induce visible cell fusion. However, as viruses can be present in absence of syncytia, rescue samples can nevertheless be harvested and transferred to fresh producer cells for potential propagation. Inefficient transfection due to poor DNA quality or unsuitable or degraded transfection reagents represent typical problems that are relatively easy to assess and remedy by generating new DNA preparations and testing different reagents, respectively.

Successful virus propagation (step 2.2) is crucially dependent on the conditions determining viral replication and cell lysis. Using low passage numbers of producer cells is recommended, and infected cells need to be regularly checked for syncytia progression. Adjusting cell numbers, temperatures, and incubation times may be required to balance viral spread vs. cell proliferation.

A crucial limitation of the described method of virus production is the preparation of virus suspensions from crude cell lysates. Researchers should be aware of the fact that the virus suspension contains cellular factors. Virus particles can be concentrated *via* density gradient/sucrose cushion ultracentrifugation at the expense of total number of infectious particles and also potentially increasing concentrations of cellular remnants. Virus can also be concentrated from infected cell supernatants, increasing purity but reducing overall yield. GMP and large scale production of paramyxoviruses is typically performed using multiple layers of producer cells seeded on a filament net in bioreactors for increased titer yield[63]. Accurate monitoring, continuous media exchange, serum-free conditions, and subsequent filtration steps ensure high purity of produced virus.

Evaluation of viral titers (steps 2.3 and 3.1) *via* the described syncytia counting method is not precise, but it is easy to perform and sufficiently accurate when using adequate numbers of technical replicates. When evaluating OV-mediated cytotoxicity (step 3.2), limitations of available assays need to be considered. Metabolic assays do not distinguish between cytostatic and cytolytic effects of experimental treatments. To measure cytolysis, an LDH release assay may be performed. However, both types of assays can be affected by contents of virus preparations from crude cell lysates (**Figure 6**).

Isolation of proteins expressed by virus-infected cells (step 4.1) can vary greatly in yield and purity, depending on the respective transgene and virus used as well as on technical accuracy. Thus, quality control of protein purification is crucial for the evaluation of related experimental results.

As an exhaustive description of potential functional assays covering the wide variety of possible immunomodulators is beyond the scope of this publication, this protocol focuses on ex vivo methodology to measure cellular cytotoxicity (step 4.3). Cellular cytotoxicity, especially by CD8+ T cells, is an important mediator of immunological tumor control in successful immunotherapies[64]. This has important implications for current immunotherapy approaches using antibodies to enhance anti-tumor immune responses in general and bispecific T cell engagers in particular. Local BTE expression by oncolytic vectors has yielded promising results in several preclinical studies, including RNA[38] and DNA viruses[65,66,67,68].

Due to the complex interactions of tumor, virus, transgene product, and host immune system in living organisms, validation of immunomodulator-encoding oncolytic vectors in cell culture as demonstrated here is not sufficient to predict therapeutic outcomes. Importantly, the proposed isolated assessment of vector and immunomodulator functions, respectively, is essential for proof of concept but fails to describe potential synergies and complex interactions within the tumor microenvironment. Testing for both toxicity and efficacy in relevant in vivo models is crucial for further development of novel recombinant vector constructs but is not easily accomplished. Immunological safety is regularly monitored in non-human primates such as macaques, and mouse models are used for biodistribution and efficacy analyses[20,69]. However, many of these models have limitations regarding the expression of virus receptors in host tissues and host permissiveness, and some only insufficiently mimic the complex interplay of OV, tumor, and the immune microenvironment. Thus, careful consideration of appropriate models is mandatory.

MV-BTE treatment has previously been evaluated in human xenograft and syngeneic mouse models. No BTE transgene products were detectable in serum of mice treated with BTE-encoding MV[38], indicating successful prevention of systemic exposure even without further attenuation of the naturally oncotropic vaccine strain virus. Local expression is crucial for OV-encoded immunomodulators which are toxic when administered systemically. If necessary, tumor specificity can be enhanced by re-targeting to cell surface markers of choice[70,71,72] and microRNA-based de-targeting for enhanced oncotropism[73,74] (reviewed by Ruiz and Russell[75]). Additional modifications may be introduced to optimize vectors for specific therapeutic uses (reviewed by Miest and Cattaneo[76]), including insertion of transgenes for diagnostic purposes[77,78] or prodrug conversion to minimize side effects of chemotherapy[79,80], introduction of safety switches[81], and targeting of tumor stroma or vasculature (e.g., via bispecific antibodies[82]).

Aside from genetic modification of the viral vector, combination regimens with chimeric antigen receptor (CAR) T cell transfer[83], chemotherapy[84,85,86], or radiotherapy[87,88,89] further augment the repertoire of OVT. As MV immunity is highly prevalent, strategies to circumvent antibody neutralization have been developed, including exchanging envelope glycoproteins for those of related paramyxoviruses[90], polymer coating of particles, using cell carriers to deliver viruses, and transient immunosuppression (reviewed by Russell et al.[6]). Further development of advanced OV immunotherapy regimens requires testing of safety and therapeutic efficacy in appropriate animal models, with patient material, and, ultimately, in controlled clinical trials.

Given the plethora of possible combinations, comprehensive testing is not feasible. Mathematical modeling can aid in prioritization of potential combination regimens as well as their respective dosing and scheduling by predicting treatment outcomes in silico (reviewed by Santiago et al.[91]). When testing efficacies of novel, rationally designed vectors, sound accompanying translational research is instrumental for a deeper understanding of underlying virological and immunological processes. This is crucial for the generation of appropriate models, information on further potential targets, and advancement in the field in general. In conclusion, firsthand insight into relevant methods of vector design, generation, and characterization in this line of work will accelerate development and support exploration of novel therapeutics for future clinical translation.

## Disclosures

C.E. Engeland is listed as co-inventor of a patent regarding RNA Viruses for Cancer Immunovirotherapy owned by Heidelberg University. J.P.W. Heidbuechel has nothing to disclose.

## Acknowledgements

These methods were established in the Virotherapy Group led by Prof. Dr. Dr. Guy Ungerechts at the National Center for Tumor Diseases in Heidelberg. We are indebted to him and all members of the laboratory team, especially Dr. Tobias Speck, Dr. Rūta Veinalde, Judith Förster, Birgit Hoyler, and Jessica Albert. This work was supported by the Else Kröner-Fresenius-Stiftung (Grant 2015_A78 to C.E. Engeland) and the German National Science Foundation (DFG, grant EN 1119/2-1 to C.E. Engeland). J.P.W. Heidbuechel receives a stipend by the Helmholtz International Graduate School for Cancer Research.

## References

1. Lichty, B. D., Breitbach, C. J., Stojdl, D. F., Bell, J.C. Going viral with cancer immunotherapy. *Nature Reviews Cancer.* **14** (8), 559-567 (2014).
2. Cassady, K. A., Haworth, K. B., Jackson, J., Markert, J. M., Cripe, T. P. To Infection and Beyond: The Multi-Pronged Anti-Cancer Mechanisms of Oncolytic Viruses. *Viruses.* **8** (2) (2016).
3. Twumasi-Boateng, K., Pettigrew, J. L., Kwok, Y. Y. E., Bell, J. C. Oncolytic viruses as engineering platforms for combination immunotherapy. *Nature Reviews Cancer.* **18** (7), 419-432 (2018).
4. Achard, C., *et al.* Lighting a Fire in the Tumor Microenvironment Using Oncolytic Immunotherapy. *EBioMedicine.* **31**, 17-24 (2018).
5. Kelly, E., Russell, S. J. History of oncolytic viruses: genesis to genetic engineering. *Molecular Therapy: The Journal of the American Society of Gene Therapy.* **15** (4), 651-659 (2007).
6. Russell, S. J., Peng, K. W., Bell, J. C. Oncolytic virotherapy. *Nature Biotechnology.* **30** (7), 658-670 (2012).
7. Russell, S. J., Peng, K. W. Oncolytic Virotherapy: A Contest between Apples and Oranges. *Molecular Therapy: The Journal of the American Society of Gene Therapy.* **25** (5), 1107-1116 (2017).
8. Seymour, L. W., Fisher, K. D. Oncolytic viruses: finally delivering. *British Journal of Cancer.* **114** (4), 357-361 (2016).
9. Chen, D. S., Mellman, I. Oncology meets immunology: the cancer-immunity cycle. *Immunity.* **39** (1), 1-10 (2013).
10. Gao, Q., Park, M. S., Palese, P. Expression of transgenes from newcastle disease virus with a segmented genome. *Journal of Virology.* **82** (6), 2692-2698 (2008).
11. Billeter, M. A., Naim, H. Y., Udem, S. A. Reverse genetics of measles virus and resulting multivalent recombinant vaccines: applications of recombinant measles viruses. *Current Topics in Microbiology and Immunology.* **329**, 129-162 (2009).
12. Matveeva, O. V., Guo, Z. S., Shabalina, S. A., Chumakov, P. M. Oncolysis by paramyxoviruses: multiple mechanisms contribute to therapeutic efficiency. *Molecular Therapy Oncolytics.* **2** (2015).
13. Suter, S.E., *et al.* In vitro canine distemper virus infection of canine lymphoid cells: a prelude to oncolytic therapy for lymphoma. *Clinical Cancer Research.* **11** (4), 1579-1587 (2005).
14. Ammayappan, A., Russell, S. J., Federspiel, M. J. Recombinant mumps virus as a cancer therapeutic agent. *Molecular Therapy Oncolytics.* **3**, 16019 (2016).
15. Schirrmacher, V. Oncolytic Newcastle disease virus as a prospective anti-cancer therapy. A biologic agent with potential to break therapy resistance. *Expert Opinion on Biological Therapy.* **15** (12), 1757-1771 (2015).
16. Saga, K., Kaneda, Y. Oncolytic Sendai virus-based virotherapy for cancer: recent advances. *Oncolytic Virotherapy.* **4**, 141-147 (2015).
17. Matveeva, O. V., Kochneva, G. V., Netesov, S. V., Onikienko, S. B., Chumakov, P. M. Mechanisms of Oncolysis by Paramyxovirus Sendai. *Acta Naturae.* **7** (2), 6-16 (2015).
18. Gainey, M. D., Manuse, M. J., Parks, G. D. A hyperfusogenic F protein enhances the oncolytic potency of a paramyxovirus simian virus 5 P/V mutant without compromising sensitivity to type I interferon. *Journal of Virology.* **82** (19), 9369-9380 (2008).
19. Engeland, C. E. *et al.* A Tupaia paramyxovirus vector system for targeting and transgene expression. *The Journal of General Virology.* **98** (9), 2248-2257 (2017).
20. Russell, S. J., Peng, K. W. Measles virus for cancer therapy. *Current Topics in Microbiology and Immunology.* **330**, 213-241 (2009).
21. Aref, S., Bailey, K., Fielding, A. Measles to the Rescue: A Review of Oncolytic Measles Virus. *Viruses.* **8** (10) (2016).
22. Demicheli, V., Rivetti, A., Debalini, M. G., Di Pietrantonj, C. Vaccines for measles, mumps and rubella in children. *The Cochrane Database of Systematic Reviews.* (2), Cd004407 (2012).
23. Radecke, F., *et al.* Rescue of measles viruses from cloned DNA. *The EMBO Journal.* **14** (23), 5773-5784 (1995).
24. Martin, A., Staeheli, P., Schneider, U. RNA polymerase II-controlled expression of antigenomic RNA enhances the rescue efficacies of two different members of the Mononegavirales independently of the site of viral genome replication. *Journal of Virology.* **80** (12), 5708-5715 (2006).
25. Russell, S.J., *et al.* Remission of disseminated cancer after systemic oncolytic virotherapy. *Mayo Clinic Proceedings.* **89** (7), 926-933 (2014).
26. Hardcastle, J., *et al.* Immunovirotherapy with measles virus strains in combination with anti-PD-1 antibody blockade enhances antitumor activity in glioblastoma treatment. *Neuro-Oncology.* **19** (4), 493-502 (2017).
27. Dispenzieri, A., *et al.* Phase I trial of systemic administration of Edmonston strain of measles virus genetically engineered to express the sodium iodide symporter in patients with recurrent or refractory multiple myeloma. *Leukemia.* **31** (12), 2791-2798 (2017).
28. Galanis, E., *et al.* Phase I trial of intraperitoneal administration of an oncolytic measles virus strain engineered to express carcinoembryonic antigen for recurrent ovarian cancer. *Cancer Research.* **70** (3), 875-882 (2010).
29. Galanis, E., *et al.* Oncolytic measles virus expressing the sodium iodide symporter to treat drug-resistant ovarian cancer. *Cancer Research.* **75** (1), 22-30 (2015).
30. Kurokawa, C., *et al.* Constitutive Interferon Pathway Activation in Tumors as an Efficacy Determinant Following Oncolytic Virotherapy. *Journal of the National Cancer Institute.* **110** (10), 1123-1132 (2018).
31. Msaouel, P., *et al.* Clinical Trials with Oncolytic Measles Virus: Current Status and Future Prospects. *Current Cancer Drug Targets.* **18** (2), 177-187 (2018).
32. Grote, D., Cattaneo, R., Fielding, A. K. Neutrophils contribute to the measles virus-induced antitumor effect: enhancement by granulocyte macrophage colony-stimulating factor expression. *Cancer Research.* **63** (19), 6463-6468 (2003).
33. Grossardt, C., *et al.* Granulocyte-macrophage colony-stimulating factor-armed oncolytic measles virus is an effective therapeutic cancer vaccine. *Human Gene Therapy.* **24** (7), 644-654 (2013).

 

34. Iankov, I. D., *et al.* Expression of immunomodulatory neutrophil-activating protein of Helicobacter pylori enhances the antitumor activity of oncolytic measles virus. *Molecular Therapy: The Journal of the American Society of Gene Therapy.* **20** (6), 1139-1147 (2012).
35. Engeland, C. E., *et al.* CTLA-4 and PD-L1 Checkpoint Blockade Enhances Oncolytic Measles Virus Therapy. *Molecular Therapy: The Journal of the American Society of Gene Therapy.* **22** (11), 1949-1959 (2014).
36. Veinalde, R., *et al.* Oncolytic measles virus encoding interleukin-12 mediates potent antitumor effects through T cell activation. *Oncoimmunology.* **6** (4), e1285992 (2017).
37. Hutzler, S., *et al.* Antigen-specific oncolytic MV-based tumor vaccines through presentation of selected tumor-associated antigens on infected cells or virus-like particles. *Scientific Reports.* **7** (1), 16892 (2017).
38. Speck, T., *et al.* Targeted BiTE expression by an oncolytic vector augments therapeutic efficacy against solid tumors. *Clinical Cancer Research.* **24** (9), 2128-2137 (2018).
39. Andtbacka, R. H., *et al.* Talimogene Laherparepvec Improves Durable Response Rate in Patients With Advanced Melanoma. *Journal of Clinical Oncology: Official Journal of the American Society of Clinical Oncology.* **33** (25), 2780-2788 (2015).
40. Ribas, A., *et al.* Oncolytic Virotherapy Promotes Intratumoral T Cell Infiltration and Improves Anti-PD-1 Immunotherapy. *Cell.* **170** (6), 1109-1119.e1110 (2017).
41. Patel, S. J., *et al.* Identification of essential genes for cancer immunotherapy. *Nature.* **548** (7669), 537-542 (2017).
42. Kimple, M. E., Brill, A. L., Pasker, R. L. Overview of affinity tags for protein purification. *Current Protocols in Protein Science.* **73**, Unit 9.9 (2013).
43. Cattaneo, R., Rebmann, G., Baczko, K., ter Meulen, V., Billeter, M. A. Altered ratios of measles virus transcripts in diseased human brains. *Virology.* **160** (2), 523-526 (1987).
44. Gutsche, I., *et al.* Structural virology. Near-atomic cryo-EM structure of the helical measles virus nucleocapsid. *Science (New York, N.Y.).* **348** (6235), 704-707 (2015).
45. Kolakofsky, D., *et al.* Paramyxovirus RNA synthesis and the requirement for hexamer genome length: the rule of six revisited. *Journal of Virology.* **72** (2), 891-899 (1998).
46. Kolakofsky, D., Roux, L., Garcin, D., Ruigrok, R. W. Paramyxovirus mRNA editing, the "rule of six" and error catastrophe: a hypothesis. *The Journal of General Virology.* **86** (Pt 7), 1869-1877 (2005).
47. Parks, C.L., *et al.* Analysis of the noncoding regions of measles virus strains in the Edmonston vaccine lineage. *Journal of Virology.* **75** (2), 921-933 (2001).
48. Molecular Cloning. In: *JoVE Science Education Database.Basic Methods in Cellular and Molecular Biology.* JoVE, Cambridge, MA (2018).
49. Bacterial Transformation: The Heat Shock Method. In: *JoVE Science Education Database.Basic Methods in Cellular and Molecular Biology.* JoVE, Cambridge, MA (2018).
50. Bergkessel, M., Guthrie, C. Colony PCR. *Methods in Enzymology.* **529**, 299-309 (2013).
51. Rota, J. S., Wang, Z. D., Rota, P. A., Bellini, W. J. Comparison of sequences of the H, F, and N coding genes of measles virus vaccine strains. *Virus Research.* **31** (3), 317-330 (1994).
52. Bankamp, B., Takeda, M., Zhang, Y., Xu, W., Rota, P. A. Genetic characterization of measles vaccine strains. *The Journal of Infectious Diseases.* **204** (Suppl 1), S533-S548 (2011).
53. Dulbecco, R., Vogt, M. Plaque formation and isolation of pure lines with poliomyelitis viruses. *The Journal of Experimental Medicine.* **99** (2), 167-182 (1954).
54. Smith, P. K., *et al.* Measurement of protein using bicinchoninic acid. *Analytical Biochemistry.* **150** (1), 76-85 (1985).
55. Bradford, M. M. A rapid and sensitive method for the quantitation of microgram quantities of protein utilizing the principle of protein-dye binding. *Analytical Biochemistry.* **72**, 248-254 (1976).
56. Separating Protein with SDS-PAGE. In: *JoVE Science Education Database.Basic Methods in Cellular and Molecular Biology.* JoVE, Cambridge, MA (2018).
57. The Western Blot. In: *JoVE Science Education Database.Basic Methods in Cellular and Molecular Biology.* JoVE, Cambridge, MA (2018).
58. Menck, K., *et al.* Isolation of human monocytes by double gradient centrifugation and their differentiation to macrophages in teflon-coated cell culture bags. *Journal of Visualized Experiments.* (91), e51554 (2014).
59. Quah, B. J., Parish, C. R. The use of carboxyfluorescein diacetate succinimidyl ester (CFSE) to monitor lymphocyte proliferation. *Journal of Visualized Experiments.* (44) (2010).
60. Gerdes, J. Ki-67 and other proliferation markers useful for immunohistological diagnostic and prognostic evaluations in human malignancies. *Seminars in Cancer Biology.* **1** (3), 199-206 (1990).
61. The Transwell Migration Assay. In: *JoVE Science Education Database.Basic Methods in Cellular and Molecular Biology.* JoVE, Cambridge, MA (2018).
62. Lim, J. F., Berger, H., Su, I. H. Isolation and Activation of Murine Lymphocytes. *Journal of Visualized Experiments.* (116) (2016).
63. Ungerechts, G., *et al.* Moving oncolytic viruses into the clinic: clinical-grade production, purification, and characterization of diverse oncolytic viruses. *Molecular Therapy Methods & Clinical Development.* **3**, 16018 (2016).
64. Fridman, W. H., Zitvogel, L., Sautes-Fridman, C., Kroemer, G. The immune contexture in cancer prognosis and treatment. *Nature Reviews Clinical Oncology.* **14** (12), 717-734 (2017).
65. Yu, F., *et al.* T-cell engager-armed oncolytic vaccinia virus significantly enhances antitumor therapy. *Molecular Therapy: The Journal of the American Society of Gene Therapy.* **22** (1), 102-111 (2014).
66. Fajardo, C. A., *et al.* Oncolytic Adenoviral Delivery of an EGFR-Targeting T-cell Engager Improves Antitumor Efficacy. *Cancer Research.* **77** (8), 2052-2063 (2017).
67. Freedman, J. D., *et al.* Oncolytic adenovirus expressing bispecific antibody targets T-cell cytotoxicity in cancer biopsies. *EMBO Molecular Medicine.* **9** (8), 1067-1087 (2017).
68. Wing, A., *et al.* Improving CART-Cell Therapy of Solid Tumors with Oncolytic Virus-Driven Production of a Bispecific T-cell Engager. *Cancer Immunology Research.* **6** (5), 605-616 (2018).
69. Myers, R. M., *et al.* Preclinical pharmacology and toxicology of intravenous MV-NIS, an oncolytic measles virus administered with or without cyclophosphamide. *Clinical Pharmacology and Therapeutics.* **82** (6), 700-710 (2007).
70. Rittner, K., Schreiber, V., Erbs, P., Lusky, M. Targeting of adenovirus vectors carrying a tumor cell-specific peptide: *in vitro.* and *in vivo.* studies. *Cancer Gene Therapy.* **14** (5), 509-518 (2007).
71. Nakamura, T., *et al.* Rescue and propagation of fully retargeted oncolytic measles viruses. *Nature Biotechnology.* **23** (2), 209-214 (2005).
72. Campadelli-Fiume, G., *et al.* Retargeting Strategies for Oncolytic Herpes Simplex Viruses. *Viruses.* **8** (3), 63 (2016).


 

73. Leber, M. F., *et al.* MicroRNA-sensitive oncolytic measles viruses for cancer-specific vector tropism. *Molecular Therapy : The Journal of the American Society of Gene Therapy.* **19** (6), 1097-1106 (2011).
74. Baertsch, M. A.*, et al.* MicroRNA-mediated multi-tissue detargeting of oncolytic measles virus. *Cancer Gene Therapy.* **21** (9), 373-380 (2014).
75. Ruiz, A. J., Russell, S. J. MicroRNAs and oncolytic viruses. *Current Opinion in Virology.* **13**, 40-48 (2015).
76. Miest, T. S., Cattaneo, R. New viruses for cancer therapy: meeting clinical needs. *Nature Reviews Microbiology.* **12** (1), 23-34 (2014).
77. Phuong, L. K., *et al.* Use of a vaccine strain of measles virus genetically engineered to produce carcinoembryonic antigen as a novel therapeutic agent against glioblastoma multiforme. *Cancer Research.* **63** (10), 2462-2469 (2003).
78. Dingli, D., *et al.* Image-guided radiovirotherapy for multiple myeloma using a recombinant measles virus expressing the thyroidal sodium iodide symporter. *Blood.* **103** (5), 1641-1646 (2004).
79. Abate-Daga, D., *et al.* Oncolytic adenoviruses armed with thymidine kinase can be traced by PET imaging and show potent antitumoural effects by ganciclovir dosing. *PLoS One.* **6** (10), e26142 (2011).
80. Ungerechts, G., *et al.* Lymphoma chemovirotherapy: CD20-targeted and convertase-armed measles virus can synergize with fludarabine. *Cancer Research.* **67** (22), 10939-10947 (2007).
81. Ketzer, P., *et al.* Artificial riboswitches for gene expression and replication control of DNA and RNA viruses. *Proceedings of the National Academy of Sciences of the United States of America.* **111** (5), E554-562 (2014).
82. Freedman, J., *et al.* Targeting T-cells to human cancer associated fibroblasts using an oncolytic virus expressing a FAP-specific T-cell engager. *Keystone Symposia & Digitell, Inc.* (2018).
83. Nishio, N., *et al.* Armed oncolytic virus enhances immune functions of chimeric antigen receptor-modified T cells in solid tumors. *Cancer Research.* **74** (18), 5195-5205 (2014).
84. Bressy, C., Benihoud, K. Association of oncolytic adenoviruses with chemotherapies: an overview and future directions. *Biochemical Pharmacology.* **90** (2), 97-106 (2014).
85. Wennier, S. T., Liu, J., McFadden, G. Bugs and drugs: oncolytic virotherapy in combination with chemotherapy. *Current Pharmaceutical Biotechnology.* **13** (9), 1817-1833 (2012).
86. Fillat, C., Maliandi, M. V., Mato-Berciano, A., Alemany, R. Combining oncolytic virotherapy and cytotoxic therapies to fight cancer. *Current Pharmaceutical Design.* **20** (42), 6513-6521 (2014).
87. Li, H., Peng, K. W., Russell, S. J. Oncolytic measles virus encoding thyroidal sodium iodide symporter for squamous cell cancer of the head and neck radiovirotherapy. *Human Gene Therapy.* **23** (3), 295-301 (2012).
88. Opyrchal, M., *et al.* Effective radiovirotherapy for malignant gliomas by using oncolytic measles virus strains encoding the sodium iodide symporter (MV-NIS). *Human Gene Therapy.* **23** (4), 419-427 (2012).
89. Mansfield, D., *et al.* Oncolytic Vaccinia virus and radiotherapy in head and neck cancer. *Oral Oncology.* **49** (2), 108-118 (2013).
90. Miest, T. S., *et al.* Envelope-chimeric entry-targeted measles virus escapes neutralization and achieves oncolysis. *Molecular Therapy: The Journal of the American Society of Gene Therapy.* **19** (10), 1813-1820 (2011).
91. Santiago, D. N., *et al.* Fighting Cancer with Mathematics and Viruses. *Viruses.* **9** (9) (2017).